

Array Configuration using Resonant-Tunneling-Diode Terahertz Oscillator Integrated with Patch Antenna

Kouhei Kasagi¹, Safumi Suzuki², and Masahiro Asada¹

¹Interdisciplinary Graduate School of Science and Engineering, Tokyo Institute of Technology, Meguro-ku, Tokyo, Japan

²Graduate School of Engineering, Tokyo Institute of Technology, Meguro-ku, Tokyo, Japan

Abstract—We proposed and fabricated an oscillator array composed of three resonant-tunneling-diode terahertz oscillators integrated with slot-coupled patch antennas, which operates without the need for Si lens. We measured the radiation pattern for single and arrayed oscillators, and calculated the output power using the integration of the pattern. The output power of a single oscillator was $\sim 15 \mu\text{W}$, while approximately three times higher output power of $\sim 55 \mu\text{W}$ was achieved at $\sim 1 \text{ THz}$ for the array configuration.

I. INTRODUCTION

Imaging is one of the characteristic applications of the terahertz (THz) waves because of the high resolution of the submillimeter scale [1]. In imaging applications, compact THz sources, which can be installed into testing systems for the detection of foreign materials in pharmaceutical drugs, food, etc., are highly desired. THz oscillators with resonant tunneling diodes (RTDs) are compact devices that can operate at room temperature, and they are good candidates for THz sources. We achieved oscillations up to 1.86 THz [2] and a high output power ($\sim 610 \mu\text{W}$) at 620 GHz [3] in RTD oscillators. However, the output power at $\sim 1 \text{ THz}$ was as small as $\sim 10 \mu\text{W}$ owing to the degradation of the negative differential conductance with increasing frequency caused by the intrinsic electron delay. In addition, a bulky hemispherical Si lens is usually required beneath the RTD oscillator to extract output power, although the output power degrades due to the reflection at the lens surface. In this work, we report an array configuration with RTD oscillators integrated with patch antennas for high output power, which operates without the need for Si lens. A relatively high output power of $\sim 55 \mu\text{W}$ was obtained at $\sim 1 \text{ THz}$ in a three-element oscillator array.

II. DEVICE STRUCTURE

Fig. 1 (a) shows the device structure of RTD oscillator integrated with a patch antenna. A planar RTD oscillator with a slot resonator is fabricated on an InP substrate, and a square patch antenna is formed on a benzocyclobutene (BCB) layer stacked on the oscillator. The RTD has a negative differential conductance, which is employed for a THz oscillation. The peak current density was $35 \text{ mA}/\mu\text{m}^2$, and the peak-to-valley current ratio was ~ 2 . The mesa area was $\sim 0.7 \mu\text{m}^2$. A 12- μm -long slot resonator is positioned directly underneath the center of the patch antenna. The slot and patch antennas are inductively coupled [4], and the output power is obtained in the upward direction from the patch antenna. In addition, to achieve resonance with the oscillation frequency, we designed the side length of the patch antenna perpendicular to the slot resonator to be approximately $\lambda/(2n_{\text{BCB}})$ long, where λ is the

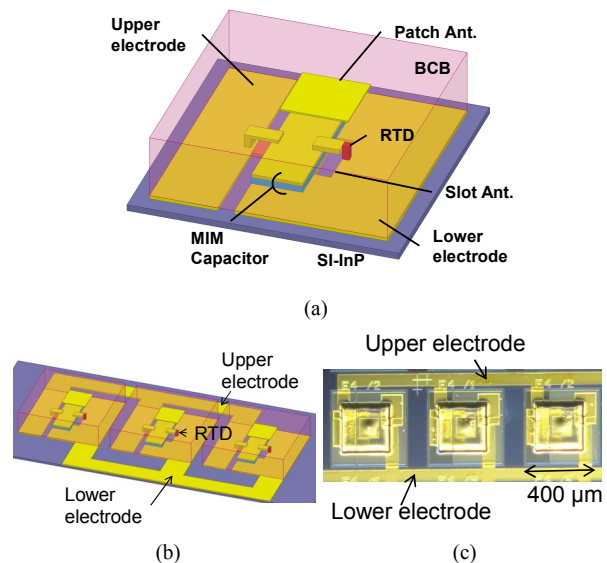


Fig. 1 (a) Device structure of single RTD oscillator integrated with patch antenna, (b) schematic structure of arrayed oscillator, and (c) micro-photograph of fabricated oscillator.

wavelength of the oscillation frequency in free space and n_{BCB} is the refractive index of the BCB layer. The side length of the patch antenna was $80 \mu\text{m}$ in this case for resonance at $\sim 1 \text{ THz}$, and the BCB was $11 \mu\text{m}$ thick. In array operation, the electrodes of single oscillators were connected in parallel, and the oscillators were simultaneously driven. Fig. 1 (b) and (c) shows the schematic structure of the three-element RTD oscillator array and a micro-photograph of the fabricated device, respectively.

III. EXPERIMENTAL RESULTS

The fabricated device was mounted on a glass slide and wire-bonded, and the radiation pattern was measured by rotating the device. For the measurement, we used a liquid-He-cooled Si-composite bolometer as the detector, which was calibrated by an Erickson power meter (PM5). Although the device can oscillate in a continuous wave mode, we performed the measurement in the pulsed mode using a lock-in technique to eliminate surrounding noise. The distance between the device and the bolometer was set to 286 mm. An iris diaphragm with a narrow aperture was inserted in front of the bolometer window to provide a high angular resolution of 1° . The transmission loss due to absorption in the atmosphere is negligible for the transmittance at $\sim 1 \text{ THz}$ and the distance between the source and detector. We also measured the radiation pattern of a single oscillator for comparison.

The measured radiation patterns in the E- and H-planes for the arrayed oscillator are shown in Fig. 2. The output power was normalized using the peak power. In the single oscillator, the full width at half maximum of the radiation pattern was $\sim 90^\circ$ and 70° for the E- and H-planes, respectively, with a single peak. In the E-plane of the arrayed oscillator, the beam width in the main lobe was narrower than that of the single oscillator, and the side lobes were observed because of the array effect of the collinearly positioned array elements. On the other hand, the beam width in the H-plane of the arrayed oscillator is almost the same as that of the single oscillator. No side lobes were observed in this direction. We also measured the radiation pattern at $\phi = 45^\circ$ and 135° for $-90^\circ < \theta < 90^\circ$, and obtained the entire radiation pattern in increments of 45° . The output power was roughly calculated by the integration of the measured radiation pattern.

Fig. 3 (a) shows the dependence of the measured output power with respect to the element number of the array. The output power of the single oscillator was $\sim 15 \mu\text{W}$, whereas combined output power of $\sim 55 \mu\text{W}$ was obtained with the arrayed oscillator. Fig. 3 (b) shows the oscillation spectrum of the arrayed oscillator having output power of $\sim 55 \mu\text{W}$. Although two peaks at 0.96 and 1.03 THz were observed owing to the imperfect locking between the elements, this is not a problem for an application to imaging because a coherent operation is not necessary.

Fig. 4 shows the output power of a single oscillator as a function of frequency for different values of $\tan\delta$ of BCB. An output power of $>100 \mu\text{W}$ is expected if $\tan\delta$ has a reported value 0.0107[5]. However, our experiments roughly fitted with the curve for $\tan\delta = 0.4$, probably because of a degradation of the BCB quality by the oxidization during the formation process. By decreasing the dielectric loss and increasing the element number of the array, higher output power is expected.

IV. CONCLUSION

We proposed and fabricated an oscillator array composed of three RTD THz oscillators integrated with slot-coupled patch antennas, which operates without the need for Si lens. We measured the radiation pattern for a single and arrayed oscillators and calculated the output power by performing an integration of the pattern. The output power of a single oscillator was $\sim 15 \mu\text{W}$, while an output power of $\sim 55 \mu\text{W}$ was obtained at $\sim 1 \text{ THz}$ in the array configuration, which is slightly higher than three times that of the single oscillator. By decreasing the dielectric loss and increasing the element number of the array, we expect to obtain a higher output power.

ACKNOWLEDGMENTS

The authors would like to thank Honorary Prof. Y. Suematsu and Prof. Emer. K. Furuya of the Tokyo Institute of Technology for their continuous encouragement. The authors would also like to thank Profs. S. Arai and Y. Miyamoto, and Assoc. Profs. M. Watanabe and N. Nishiyama of the Tokyo Institute of Technology for fruitful discussions and encouragement. This work was supported by a Scientific Grants-in-Aid from the

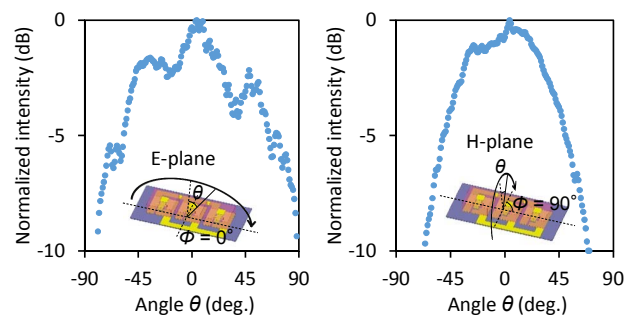


Fig. 2 Measured radiation pattern of arrayed oscillator for E- and H-planes.

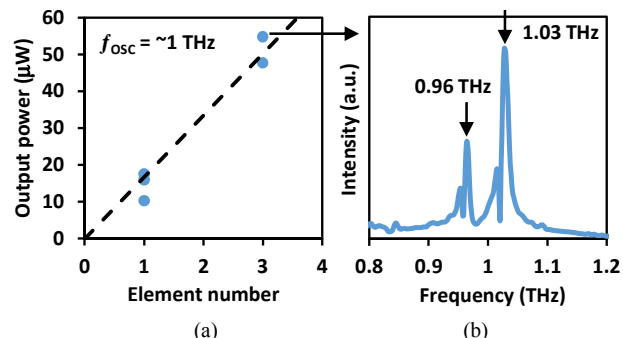


Fig. 3 (a) Measured output power vs. number of elements; (b) frequency spectrum of oscillator array obtained at $\sim 55 \mu\text{W}$.

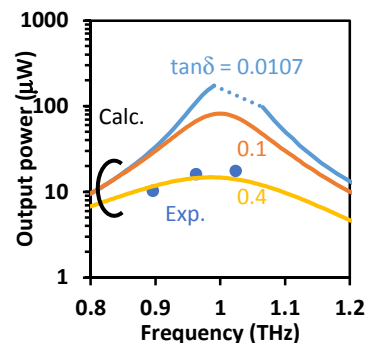


Fig. 4 Output power as a function of oscillation frequency for different dielectric losses of BCB.

Ministry of Education, Culture, Sports, Science and Technology, Japan, the Industry–Academia Collaborative R&D Program from the Japan Science and Technology Agency, and the Strategic Information and Communications R&D Promotion Programme (SCOPE) from the Ministry of Internal Affairs and Communications, Japan.

REFERENCES

- [1]. W. L. Chan, J. Deibel, and D. M. Mittleman, "Imaging with terahertz radiation," *Rep. Prog. Phys.*, vol. 70, pp. 1325–1379, 2007
- [2]. H. Kanaya, T. Maekawa, S. Suzuki, and M. Asada, *TeraNanoV*, Martinique, Dec, 2014.
- [3]. S. Suzuki, M. Shiraishi, H. Shibayama, and M. Asada, *IEEE J. Sel. Top. Quantum Electron.*, vol. 19, no. 1, 8500108, 2013.
- [4]. M. Himdi, J. P. Daniel, and C. Terret, "Transmission line analysis of aperture-coupled microstrip antenna," *Electron. Lett.*, vol. 25, no. 18, pp. 1229–1230, Aug. 1989.
- [5]. E. Perret, N. Zerounian, S. David, and F. Aniel, *Microelectronic Engineering*, vol. 85, pp. 2276–2281, 2008.